PERFORMANCE OF THREE-DIMENSIONAL SLOPE STABILITY METHODS IN PRACTICE

By Timothy D. Stark[1] and Hisham T. Eid,[2] Associate Members, ASCE

ABSTRACT: Study of several field case histories has shown that the difference between two- and three-dimensional factors of safety is most pronounced in cases that involve a translational failure. Two- and three-dimensional slope stability analyses of field case histories and a parametric study of a typical slope geometry revealed that commercially available three-dimensional slope stability programs have a number of limitations with respect to (1) accounting for the shear resistance along the sides of the sliding mass; (2) modeling the stress-dependent nature of failure envelopes of the materials involved; and (3) considering the internal forces in the slide mass. These limitations can significantly affect the calculated factor of safety for a translational failure mode. A technique is presented to overcome some of these limitations and provide a better estimation of the three-dimensional factor of safety. Field case histories are presented to show the importance of using a three-dimensional analysis in back-calculating the mobilized shear strength of the materials involved in a slope failure and in the design of slopes with complicated topography, shear strength conditions, and/or pore-water pressures.

INTRODUCTION

At present, most slope stability analyses are performed using a two-dimensional (2D) limit equilibrium method. These methods calculate the factor of safety against failure for a slope assuming a plane-strain condition. Therefore, it is implicitly assumed that the failure surface is infinitely wide, and thus three-dimensional (3D) effects are negligible because of the infinite width of the slide mass. Clearly, slopes are not infinitely wide and 3D effects influence the stability of most, if not all, slopes. In general, the 2D analysis is appropriate for slope design because it yields a conservative estimate for the factor of safety (Duncan 1992). It is conservative because the end effects are not included in the 2D estimate of the factor of safety. A 3D analysis is recommended for back-analysis of slope failures so that the back-calculated shear strength reflects the 3D end effects. The back-calculated shear strength then can be used in remedial measures for failed slopes or slope design at sites with similar conditions.

Skempton (1985) suggested applying the following three-dimensional correction factor to the shear strength back-calculated from a two-dimensional analysis:

$$\frac{1}{1 + \frac{KD}{B}} \tag{1}$$

where K = coefficient of earth pressure mobilized at failure; D = average depth of the failure mass; and B = average width of the failure mass. Skempton (1985) also reported that this correction factor usually results in a 5% increase in the back-calculated shear strength. However, this 5% correction is an average value, and varies for different cases and material types. It will be shown herein that the percentage can be as large as 30%, and thus a three-dimensional analysis should be conducted to back-calculate the shear strengths mobilized along a known failure surface.

A number of 3D slope stability methods and computer programs have been developed. The validity of the analytical results depends on the degree to which the analysis matches the field mechanics, and on the success of the user in modeling the field geometry and engineering properties with the program. Most of the existing 3D slope stability methods and computer programs have been evaluated using parametric studies and not field case histories [e.g., Chen and Chameau (1983); Lovell (1984); Thomaz and Lovell (1988)]. Therefore, a widely accepted 3D stability analysis is not yet available for practicing geotechnical engineers. Through analysis of well-documented field case histories, the present paper introduces the site conditions in which a 3D stability analysis is most important, investigates the accuracy of available 3D stability methods and software, presents a technique to improve this accuracy, and, finally, provides a comparison of 2D and 3D analyses.

FAILURE MODE FOR 3D SLOPE STABILITY STUDY

To achieve the prior objectives, case histories that involve translational failure through an underlying weak material(s), such as a cohesive soil and/or geosynthetic interface, were studied. This type of failure was chosen for the following reasons:

1. Slopes failing in a translational mode usually involve either a significantly higher or lower mobilized shear strength along the back scarp and sides of the slide mass than that along the base, e.g., the upstream slope failure in Waco Dam (Beene 1967; Wright and Duncan 1972) and the slope failure in Kettlemen Hills hazardous waste repository (Seed et al. 1990; Byrne et al. 1992; Stark and Poeppel 1994), respectively. These situations can result in a significant difference between the 2D and 3D factors of safety. This difference is less pronounced in slopes that fail in a rotational mode, which usually occurs in homogeneous materials (Fig. 1).
2. A translational failure can occur in relatively flat slopes because of the weak nature of the underlying material(s). The flatter the slope, the greater the difference between the 2D and 3D factors of safety (Chen and Chameau 1983; Leshchinsky et al. 1985).
3. The end effects are more pronounced for slopes of cohesive materials (Chen 1981; Lovell 1984; Leshchinsky and Baker 1986; Ugai 1988).
4. A translational failure often involves a long and nearly horizontal sliding plane through a preexisting failure surface along which a residual shear strength condition is mobilized in soils [e.g., Maymont slide (Krahn et al. 1979), Gardiner Dam movement (Jasper and Peters 1979), and Portuguese Bend slide (Ehlig 1992)]. If geo-

[1]Assoc. Prof. of Civ. Engrg., Univ. of Illinois, Newmark Civ. Engrg. Lab. MC-250, 205 N. Mathews Ave., Urbana, IL 61801-2352.

[2]Postdoctoral Res. Assoc. of Civ. Engrg., Univ. of Illinois, Urbana, IL.

Note. Discussion open until April 1, 1999. To extend the closing date one month, a written request must be filed with the ASCE Manager of Journals. The manuscript for this paper was submitted for review and possible publication on January 16, 1998. This paper is part of the ***Journal of Geotechnical and Geoenvironmental Engineering***, Vol. 124, No. 11, November, 1998. ©ASCE, ISSN 1090-0241/98/0011-1049–1060/ $8.00 + $.50 per page. Paper No. 17399.

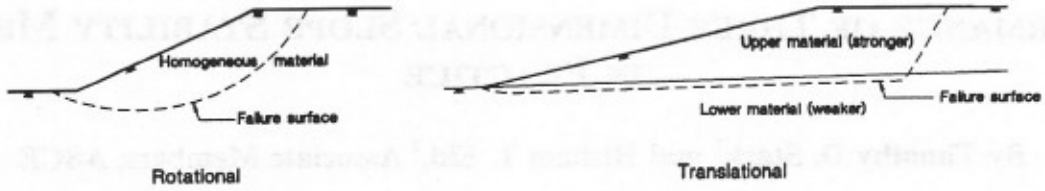

FIG. 1. Two Different Failure Modes for Slopes

synthetics are involved, a translational failure may occur without mobilizing a postpeak shear strength condition along the entire failure surface because of the low strength of some geosynthetic interfaces, e.g., Kettlemen Hills repository. The presence of a preexisting failure surface or weak interface in these cases can provide some certainty in the shear strength input data. In contrast, a rotational failure in homogeneous material usually involves a progressive failure mechanism that may lead to a poor estimation of the mobilized shear strength (Eid 1996).

5. A translational failure often involves a drained shearing condition. This facilitates estimation of the mobilized shear strength of the materials involved because excess pore-water pressures do not have to be estimated.
6. A three-dimensional stability analysis is generally needed to back-calculate the mobilized shear strength of the materials involved in a slope failure for use in remedial measures or design of slopes at sites with similar geotechnical characteristics. This is common after a translational failure.

THREE-DIMENSIONAL SLOPE STABILITY SOFTWARE

Commercially available 3D slope stability software was studied to investigate the ability of the software to calculate an accurate 3D factor of safety. The studied software includes 3D-PCSTABL (Thomaz 1986), CLARA 2.31 (Hungr 1988), and TSLOPE3 (Pyke 1991). The following 3D stability software was also investigated, but the limitation of a 3D shear surface with only a cylindrical shape precluded its use in the study: STAB3D (Baligh and Azzouz 1975), LEMIX-&FESPON (Chen and Chameau 1983), BLOCK3 (Lovell 1984), and F3SLOR&DEEPCYL (Gens et al. 1988). Several case histories were analyzed using 3D-PCSTABL, CLARA 2.31, and TSLOPE3 to study the effect of their capabilities and limitations in describing the slope geometry, pore-water pressure conditions, modeling of the material shear strength behavior, and calculation of the minimum 3D and 2D factors of safety. Table 1 gives a brief description of the main differences between the software for analyzing a translational slope failure.

As shown in Table 1, 3D-PCSTABL can only be used in the analysis of slopes with a symmetrical failure surface. This limitation prevents the use of this software for most translational failures because the failure surface is usually asymmetrical in both the horizontal and the vertical direction. CLARA 2.31 and TSLOPE3 can analyze slopes with any shape of failure surface. However, CLARA 2.31 satisfies more conditions of equilibrium, utilizes different methods of 3D analysis, and is more user-friendly than is TSLOPE3. In addition, CLARA 2.31 has more capability in describing piezometric surfaces and external loads. As a result, CLARA 2.31 was used for all 3D and some 2D stability analyses described in the present paper. It should be noted that all of the available 3D slope stability software assumes that the whole sliding mass moves in the same direction; i.e., the direction of sliding is uniform for the entire mass. Consequently, this assumption was also applied to the 3D stability analyses described in the current paper.

CLARA 2.31 utilizes either an extension of Bishop's simplified method or Janbu's simplified method to three dimensions (Hungr 1987). The assumptions required to render the 3D analysis statically determinate are the same as those for the 2D methods (Bishop 1955; Janbu et al. 1956). In extending Bishop's simplified method, the intercolumn shear forces are assumed to be negligible, and the vertical force equilibrium of each column and the overall moment equilibrium of the column assembly are sufficient conditions to determine all of the unknowns. Horizontal force equilibrium in both the longitudinal and the transverse direction is neglected. The factor of safety equation is derived from the sum of moments about a common horizontal axis parallel to the x-direction. Janbu's simplified method assumes that conditions of horizontal and vertical force equilibrium are sufficient to determine all unknowns, and therefore, moment equilibrium is not satisfied. The factor of safety equation is derived from the horizontal force equilibrium equation. Fig. 2 shows the forces acting on a typical column used in CLARA 2.31.

PARAMETRIC STUDY

The 3D factor of safety can be poorly estimated using commercially available software because of limitations in describing the slope geometry, material properties, and/or limitations in the analysis methods. The effect of these limitations on the calculated 3D factor of safety was studied using a model of a typical translational failure. A number of field case histories that experienced a translational failure were used to design the slope model so that it simulates field conditions with respect to slide mass dimensions (ratio between average depth and width), ground surface, side and base slope inclinations, and material unit weights and shear strengths. Fig. 3 shows a plan view and a representative cross section of this model.

Fig. 4 shows the assumed shear strength envelopes of the two materials involved in the slope model analysis. The ratio in shear strength between the upper and lower materials is taken to simulate the ratio between the peak shear strength of a stiff fissured clay mass, i.e., the fully softened shear strength, and the residual shear strength of the same clay, respectively (Stark and Eid 1997). A liquid limit and clay-size fraction of 95% and 50%, respectively, were assumed and used to estimate the shear strength values (Stark and Eid 1994, 1997). This shear strength ratio can also approximately simulate the ratio between the peak shear strength of municipal solid waste (Kavazanjian et al. 1995; Stark et al. 1998) and the residual shear strength of a geosynthetic interface in the underlying composite liner system in a landfill (Stark et al. 1996). The saturated unit weights of the upper and lower materials were assumed to be 17 and 18 kN/m^3, respectively. Fig. 4 also shows two linear approximations of the failure envelopes. Linear failure envelopes passing through the origin and the shear strength corresponding to the average effective normal stress on the slip surfaces yield friction angles of 23° and 8° for the upper and lower materials, respectively. The effect of using this approximation and the actual failure envelope on the calculated 3D factor of safety is discussed in a subsequent section of this paper.

TABLE 1. Main Differences between Commercially Available 3D Slope Stability Software for Analyzing Translational Slope Failures

Program name (1)	Theoretical bass for 3D method (2)	Statical assumptions (3)	Equilibrium condition satisfied (4)	Shape of failure surface (5)	Piezometric pressure specification (6)	Number of possible piezometric surfaces (7)	Shear strength models (8)	Calculating yield seismic coefficient (9)	Accommodating external loads (10)	Search for direction of minimum FS for certain failure mass (11)	Search for 3D critical failure surface (12)	2D analysis out of 3D data file (13)	Creating data file (14)
CLARA 2.31 (Hungr 1988)	Bishop's simplified method or Janbu's simplified method	Vertical intercolumn shear forces are zero	Vertical force and moment	Any	Hydrostatic or using pore-pressure ratio "r_u"	Several	Linear Mohr-Coulomb envelope or parabolic envelope [proposed by Hoek and Brown (1980)]	Yes	Yes	Yes	Yes (for circular surface only)	Yes	Using an interaction interface
TSLOPE3 (Pyke 1991)	Los Angeles County method	Intercolumn forces are zero	Horizontal force	Any	Hydrostatic	One	Linear or nonlinear Mohr-Coulomb envelope or parabolic envelope [proposed by Hoek and Brown (1980)]	Yes	No	Yes	No	Yes	Using an editor or word processor
3D-PCSTABL (Thomaz 1986)	Method of slices	Interslice forces on the sides of the column have the same inclination; intercolumn shear forces are parallel to the column base	All forces and moments	Symmetrical	Hydrostatic or using pore-pressure ratio "r_u"	Several	Linear Mohr-Coulomb envelope	Yes	No	No	Yes	No	Using routine interface or word processor

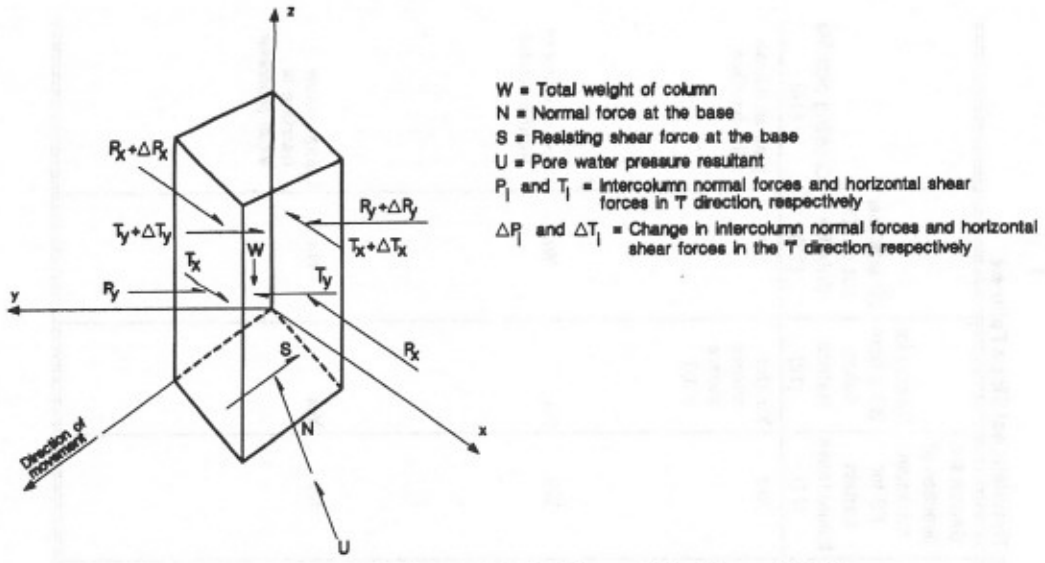

FIG. 2. Forces Acting on Single Column [after Hungr (1987)]

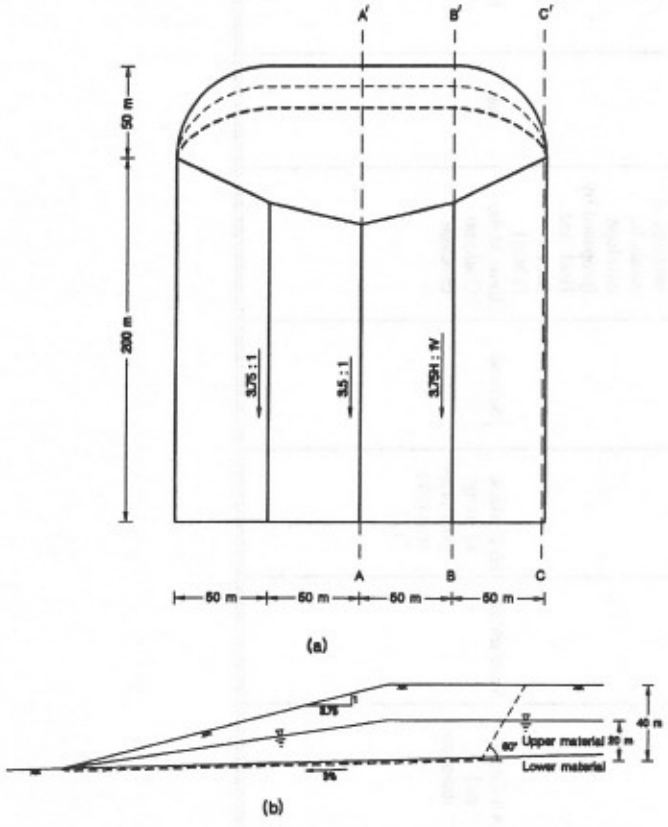

FIG. 3. Plan View and Representative Cross Section for Slope Model: (a) Plan View; (b) Cross Section B-B'

It should be noted that the sides of the slide mass in the slope model are vertical. In translational failures, vertical sides provide the minimum amount of shear resistance because the effective normal stress acting on these sides is only due to the lateral earth pressure and a vertical side produces the minimum area of shear surface. A translational failure with inclined sides usually occurs if inclined weak surfaces are present along the sides of the slide mass. This was the case in the slope failure at the Kettlemen Hills hazardous waste repository.

The slope stability software divides the slide mass up into vertical columns. The user selects a grid spacing that is used to place a grid over the basal surface and to define the vertical columns into which the potential sliding mass is subdivided for the analysis. These columns are the 3D equivalent of the vertical slices used in a conventional 2D analysis. The resisting forces are calculated by considering the material shear strength along the base of each column. As a result, the shear resistance due to cohesion and/or friction generated by the earth pressure on the sides of the vertical columns along the vertical sides of the slide mass is ignored (Fig. 5). This usually leads to an underestimation of the 3D factor of safety, especially when the material along the vertical sides has a higher shear strength than the material along the base of the slide mass. An example of this could be a failure surface that extends through municipal solid waste to an underlying material that involves a weak soil or geosynthetic interface in the liner system.

Two- and three-dimensional analyses were performed for the slope model to study the effect of ignoring the shear resistance along the vertical sides, using a linear approximation for a stress dependent failure envelope of the materials involved, and using different slope stability methods or assumptions on the calculated 3D factor of safety. Table 2 shows the calculated 2D and 3D factors of safety for various analysis conditions. It should be noted that while CLARA 2.31 was used for the 3D analyses, both CLARA 2.31 and UTEXAS3 (Wright 1992) slope stability programs were used to calculate the 2D factors of safety. UTEXAS3 was used to verify the calculated factors of safety and incorporate a nonlinear failure envelope in the 2D analysis by inputting combinations of shear and normal stresses to describe the failure envelope.

Effect of Shearing Resistance along Vertical Sides of Slide Mass

As described previously, the available 3D stability software does not consider the shear resistance along the vertical sides of the sliding mass in calculating the 3D factor of safety. To include this side resistance, a change in the input data was made so that a shear force equivalent to the side resistance is used in calculating the factor of safety. This was accomplished for the slope model by using an "imaginary" material layer that surrounds only the sides of the slide mass. As a result, the material properties of this layer affect only the shear strength along the vertical sides, and not the back scarp or base of the sliding mass. This layer has a unit weight equal to that of the upper material; a friction angle, ϕ_i', of zero; and cohesion, c_i', equal to the shear strength due to the at-rest earth pressure acting on the vertical sides of the slide mass. The cohesion can be estimated using the following equation:

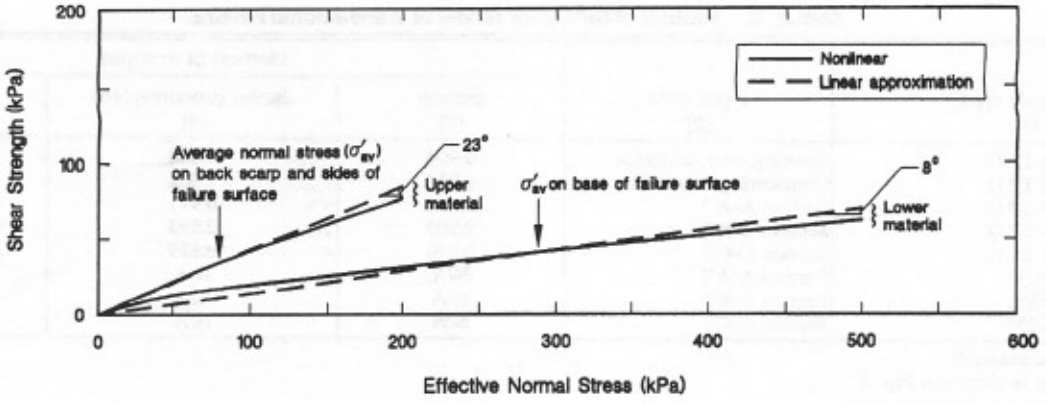

FIG. 4. Shear Strength Envelopes Used for 3D Slope Model Analyses

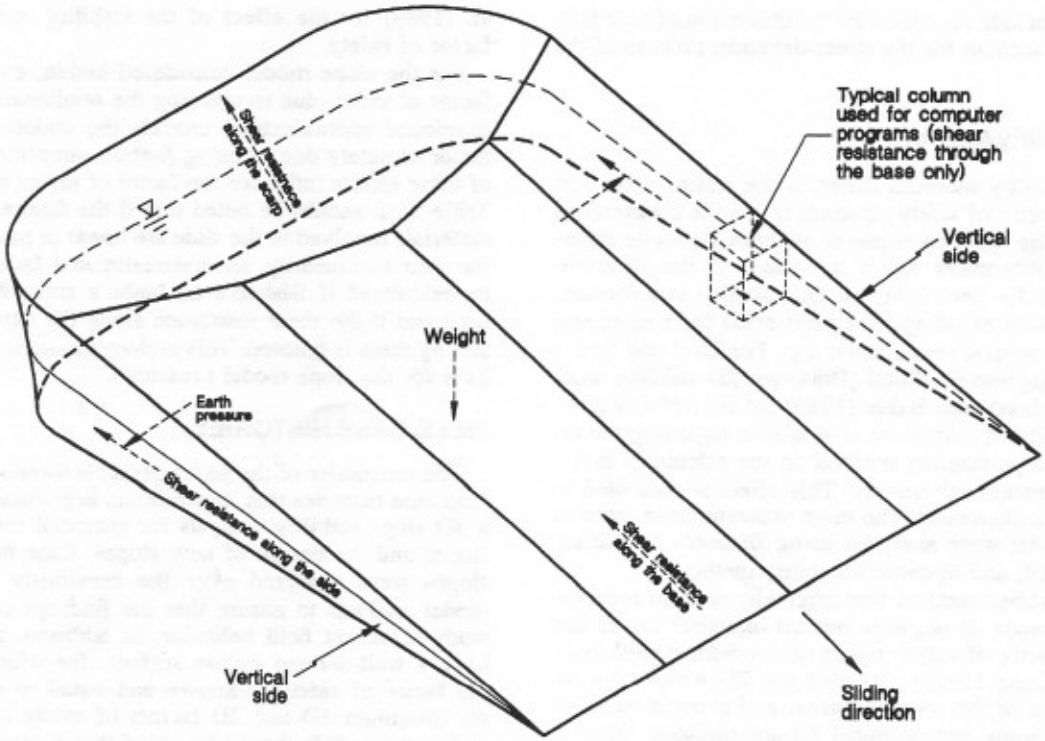

FIG. 5. 3D View of Slope Model

$$c'_i = k_0 \sigma'_v \tan \phi' \quad (2)$$

where ϕ'_v = average vertical effective stress over the depth of the sliding mass side; ϕ' = secant friction angle of the upper material corresponding to the approximated average effective normal stress on the vertical sides of the sliding mass; and k_0 = coefficient of earth pressure at rest for the upper layer material ($k_0 = 1 - \sin \phi'$). In addition to using the imaginary layer, a slight (less than 5°) outward inclination is assigned to each vertical side of the sliding mass to include a single column so that the software can consider the effect of cohesion in the shear resistance calculations. No resisting or driving force is mobilized due to the weight of this column because the friction angle of the imaginary layer is assumed to be zero.

The first two rows in Table 2 show that for the slope model considered herein, including the vertical side resistance increases the calculated 3D factor of safety by about 13% using both Bishop's and Janbu's simplified methods. The side resistance effect increases with increasing difference between the shear strength of the upper and lower layers. Table 2 also indicates that if the resistance along vertical sides is ignored, i.e., no side resistance, the calculated 3D factor of safety is approximately equal to the average of the 2D factors of safety through the sliding mass, i.e., for sections A-A′, B-B′, and C-C′.

Importance of Failure Envelope Nonlinearity

Nonlinear failure envelopes and their linear approximations shown in Fig. 4 were used to calculate the 2D factor of safety for different cross sections of the slope model using Spencer's stability method (Spencer 1967). Each stress-dependent failure envelope was modeled using 19 shear and normal stress combinations in UTEXAS3 (Wright 1992). Results in Table 2 show that ignoring the nonlinearity of the failure envelope, i.e., using a linear failure envelope that passes through the origin and the shear strength corresponding to the average effective normal stress on the slip surface, leads to an overestimation of the 2D factors of safety of less than 10%. For example, ignoring the nonlinearity of the failure envelope in the analysis of cross section A-A′ increases the calculated 2D factor of safety from 0.909 to 0.987. A similar effect is expected for the 3D factor of safety. The effect of ignoring the nonlinearity of the failure envelope should increase with an increase in the range of effective normal stress acting on the slip surface. As a result, it is recommended that 3D slope sta-

TABLE 2. Factors of Safety for Model of Translational Failure

Analysis type (1)	Input data (2)	Method of Analysis: Bishop (3)	Janbu (uncorrected) (4)	Spencer (5)
3D (using CLARA 2.31)	Ignoring side resistance	0.900	0.888	N/A
3D (using CLARA 2.31)	Considering side resistance	1.014	1.001	N/A
2D (using CLARA 2.31)	Section A-A'[a]	0.924	0.911	0.987
2D (using CLARA 2.31)	Section B-B'[a]	0.905	0.893	0.966
2D (using CLARA 2.31)	Section C-C'[a]	0.870	0.859	0.929
2D (using UTEXAS3)	Section A-A'[a]	N/A	N/A	0.987 (0.909)[b]
2D (using UTEXAS3)	Section B-B'[a]	N/A	N/A	0.966 (0.890)[b]
2D (using UTEXAS3)	Section C-C'[a]	N/A	N/A	0.929 (0.856)[b]

Note: N/A = not available.
[a]Section location is shown in Fig. 3.
[b]Nonlinear failure envelope was used.

bility software include an option for inputting a nonlinear failure envelope to account for the stress-dependent nature of the shear strength.

3D Slope Stability Methods

The slope stability methods differ in the statics employed in deriving the factor of safety equation and in the assumptions used to render the limit equilibrium analysis statically determinate. These differences affect the value of the factor of safety calculated for each method. Quantitative comparisons of computed factors of safety have been made for a rotational failure mode by several researchers; e.g., Fredlund and Krahn (1977), and Ching and Fredlund (1984) for 2D stability analysis, and Leshchinsky and Baker (1986) for 3D stability analysis. However, little information is available regarding the effect of the 3D slope stability method on the calculated factor of safety for translational failures. This effect is presented in Table 2 using the 2D results. The three different cross sections of the slope model were analyzed using Bishop's simplified, Janbu's simplified, and Spencer's stability methods.

Bishop's simplified method was originally derived for a rotational failure mode. It neglects vertical interslice forces and calculates the factor of safety based on moment equilibrium. Fredlund and Krahn (1977) extended the 2D method by including moments of the normal forces, and showed satisfactory results for some nonrotational failure surfaces. Since it neglects the internal shear strength in the vertical direction, Bishop's simplified method underestimates the factor of safety calculated using Spencer's method (Table 2). Janbu's simplified method assumes that the resultant interslice forces are horizontal, and uses an empirical correction factor to account for the interslice vertical force. The factor of safety is calculated based on force equilibrium. If the correction factor is not used, Janbu's simplified method also underestimates the factor of safety calculated using Spencer's method. Spencer's method assumes that the resultant interslice forces have the same inclination throughout the sliding mass. Both force and moment equilibrium are satisfied in Spencer's method. This method is regarded as being accurate, i.e., within 6% of the correct 2D factor of safety (Duncan 1992). This is especially true for the translational failure mode in which the inclination of the interslice force in the major part of the slope is nearly constant.

Comparing the 2D factors of safety calculated using these three stability methods presented in Table 2 shows that Bishop's and Janbu's simplified methods underestimate the factor of safety calculated using Spencer's method by approximately 6% and 8%, respectively, for the slope model. Underestimating the factor of safety increases with an increasing difference between the shear strength of the upper material, i.e., internal shear strength, and the shear strength along the sliding surface. A similar conclusion was reached by Hungr et al. (1989) for the effect of the stability method on the 2D factor of safety.

For the slope model considered herein, overestimating the factor of safety due to ignoring the nonlinearity of the failure envelopes approximately cancels the underestimation of the factor of safety due to using Janbu's simplified method. Both of these effects influence the factor of safety by about 8% (see Table 2). It should be noted that if the failure envelope of the materials involved in the slide are linear or modeled to account for their nonlinearity, an underestimated factor of safety will be calculated if Bishop's or Janbu's simplified methods are used and if the shear resistance along the vertical sides of the sliding mass is ignored. This underestimation is approximately 21% for the slope model presented.

FIELD CASE HISTORIES

The remainder of the paper presents three well-documented field case histories that illustrate the importance of performing a 3D slope stability analysis for remedial measures of failed slopes and the design of new slopes. Case histories of failed slopes were analyzed after the previously described slope model analysis to ensure that the findings of the parametric study represent field behavior. In addition, the failed slopes have a well-defined failure surface, for which the minimum 3D factor of safety is known and equal to unity. Therefore, the minimum 3D and 2D factors of safety can be calculated and compared. It should be noted that a comparison between 3D and 2D factors of safety for a particular slope is only meaningful when the minimum factors of safety are compared (Cavounidis 1987). The parameters that were studied in the analysis of the hypothetical slope model are considered in the analysis of the field case histories. The case histories utilized English units, and thus English units are used in the text and figures, with metric equivalents presented in parentheses.

San Diego Landslide

The 1979 Oceanside Manor landslide occurred along a bluff approximately 65 ft (20 m) high in a residential area in San Diego County, California. The length of the scarp is approximately 430 ft (130 m), and the slide encompassed approximately 160,000 cu yd (122,000 m^3) of soil. Figs. 6 and 7 show a plan view and a representative cross section of the landslide, respectively, prior to failure. The slope is underlain by the Santiago Formation. At this site, the Santiago Formation is composed of a claystone and a sandstone. The sandstone is fine-to-medium grained and overlies the gray claystone. The remolded claystone classifies as a clay or silty clay of high plasticity, CH-MH, according to the Unified Soil Classification System. The liquid limit, plasticity index, and clay-size fraction are 89, 45, and 57%, respectively (Stark and Eid 1992).

Field investigation showed that the claystone is commonly

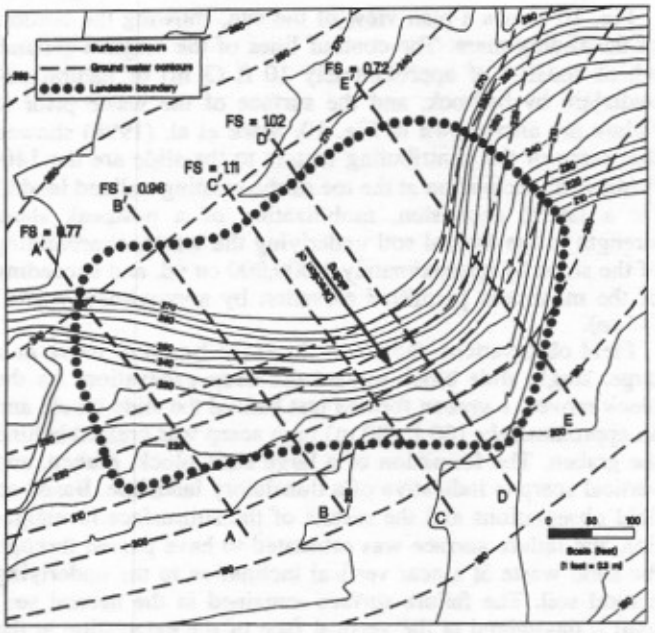

FIG. 6. Plan View of San Diego Landslide

fissured, displaying numerous slicken sided surfaces. The site has undergone at least three episodes of landsliding prior to the slide that is back-calculated in the present paper. Therefore, the claystone has undergone substantial shear displacement and has probably reached a residual strength condition along the base of the sliding surface. In addition, the largest portion of the sliding surface in the claystone is approximately horizontal through the Santiago Formation. This indicates that sliding probably occurred along a weak claystone seam or layer. As a result, residual and fully softened shear strengths were assumed to be mobilized during failure along the base and the scarp, respectively, in the Santiago Formation (Stark and Eid 1994, 1997). The slide surface was located using slope inclinometers and extensive borings and trenches. The groundwater levels were extensively monitored using piezometers, and water levels in borings and trenches shortly after movement started to occur. This resulted in the ground-water contours shown in Fig. 6.

A three-dimensional slope stability analysis was conducted for the sliding mass shown in Fig. 8. The sides of the sliding mass were taken to be nearly vertical. In addition, the back scarp was assumed to be inclined 60° from the horizontal to simulate an active earth pressure condition. These failure surface conditions result in a minimum sliding resistance during slope failure. The moist unit weight of the Santiago claystone and the compacted fill were measured to be 125 pcf (19.6 kN/m^3). Residual and fully softened shear strengths of the Santiago claystone were measured using the ring shear test procedure described by Stark and Eid (1993, 1997). The resulting residual and fully softened failure envelopes were approximated by linear failure envelopes that pass through the origin and the average effective normal stress acting on the sliding mass base and sides, respectively. This leads to an average residual friction angle of 7.5° and an average fully softened friction angle of 22.5°. It should be noted that the fully softened friction angle of the claystone along the back scarp was used for calculating the mobilized shear strength of the sliding mass. The fully softened friction angle was taken to be 25° (2.5° higher than the value measured using the ring shear apparatus) to account for the triaxial compression mode of failure instead of the ring shear failure mode (Stark and Eid 1997). The cohesion and friction angle of the compacted fill were measured, using direct shear tests, to be zero and 26°, respectively.

For the sliding mass shown in Fig. 8, a 3D slope stability analysis using Janbu's simplified method yielded a factor of safety of 0.94. The shear resistance along the sides of the slide

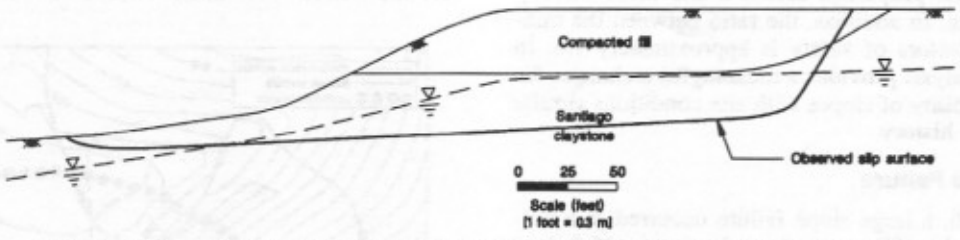

FIG. 7. Cross Section and 2D Failure Surface of San Diego Landslide (Section D-D')

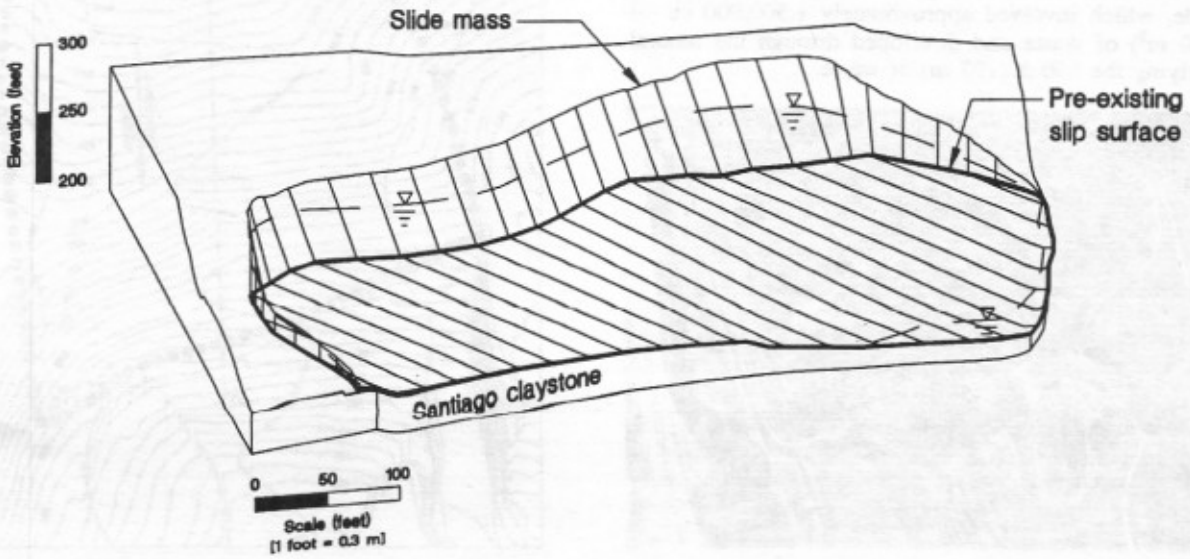

FIG. 8. 3D View of Slide Mass for San Diego Landslide

mass was not considered by the CLARA 2.31 software in this calculated factor of safety. This 3D factor of safety is slightly higher than the average 2D factors of safety of 0.92 that was calculated for 44 different cross sections in the direction of movement through the sliding mass. The location and factor of safety for five representative cross sections are shown in Fig. 6. As discussed before, if side resistance is not included, the calculated 3D factor of safety is close to the average 2D factor of safety for representative cross sections. It should also be noted that the calculated factor of safety of 0.94 is less than a factor of safety of unity that is expected for a slope at a state of incipient failure.

For the representative 2D cross sections, overestimating the factor of safety due to ignoring the nonlinearity of the failure envelopes approximately cancels the underestimation of the factor of safety due to using Janbu's simplified method. As a result, the main source of error in calculating the 3D factor of safety for this case is ignoring the shear resistance along the vertical sides of the slide mass. The slope was reanalyzed to include the shear resistance along the vertical sides of the slide mass using the technique involving (2). The coefficient of earth pressure and the friction angle used in calculating the cohesion of the imaginary layer in (2) are 0.58 and 25°, respectively. The reanalysis yielded a 3D factor of safety of 1.02. This represents about a 9% increase in the calculated 3D factor of safety due to incorporating the side resistance. This increase is significant, considering the relatively small area of the vertical sides of the sliding mass (Fig. 8). However, the large difference between the mobilized friction angle along the base of the slide mass (7.5°) and vertical sides (25°) enhanced the effect of the side resistance on the overall calculated 3D factor of safety.

The 2D factors of safety vary significantly according to the cross section location because of the variations in topography and ground-water level over the sliding area (Fig. 6). A 3D analysis can accommodate variations in geometry, pore-water pressure, and material properties across a site more directly than can 2D analyses. In addition, the ratio between the minimum 3D and 2D factors of safety is approximately 1.6. In summary, the 3D analysis provides a meaningful technique for investigating the stability of slopes with site conditions similar to those in this case history.

Cincinnati Landfill Failure

On March 9, 1996, a large slope failure occurred in a municipal solid waste landfill approximately 9 mi (15.3 km) northeast of Cincinnati, Ohio. Fig. 9 is an aerial view of the waste slide, which involved approximately 1,500,000 cu yd (1,000,000 m^3) of waste and developed through the natural soil underlying the 350 ft (107 m) of waste.

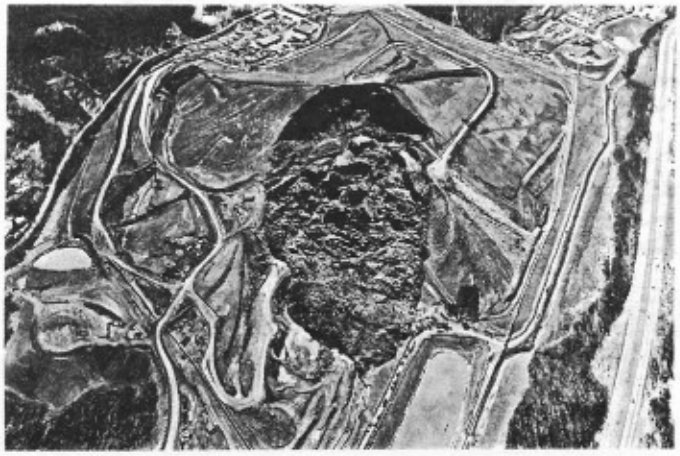

FIG. 9. Aerial View of Cincinnati Landfill Failure

Fig. 10 shows a plan view of the site, showing the borders of the sliding mass. The contour lines of the original ground, which consists of approximately 10 ft (3 m) of natural soil underlain by bedrock, and the surface of the waste prior to failure are also shown in Fig. 10. Stark et al. (1998) showed that some of the contributing factors to the slide are the 140-ft (42.7 m) excavation at the toe of the existing unlined landfill for a lateral expansion, mobilization of a postpeak shear strength in the natural soil underlying the waste, overbuilding of the slope by approximately 1,000,000 cu yd, and exceeding of the maximum permitted elevation by approximately 50 ft (15 m).

Field observations show that the slope began to move as a large, single slide block toward the deep excavation. As the block moved, a graben formed just behind the slide block, and an approximately 100 ft (30 m) high scarp was created behind the graben. The formation of a large slide block, graben, and vertical scarp is indicative of a translatory landslide. Based on field observations and the results of the subsurface investigation, the failure surface was estimated to have passed through the solid waste at a near vertical inclination to the underlying natural soil. The failure surface remained in the natural soil, until it daylighted at the vertical face of the excavation at the toe of the slope (Fig. 11).

Determining the mobilized shear strength of the natural soil in this case was important for the design of the reconstructed slope, and the design of other interim and permanent slopes that involve similar soil. Stark et al. (1998), using published data from large direct shear box testing, the height of the vertical back scarp and active earth pressure theory, and other case histories, estimated the cohesion and friction angle of the solid waste to be 845 psf (41 kPa) and 35°, respectively. Moist unit weight of the solid waste was estimated to be 65 pcf (10.2 kN/m^3). To back-calculate the mobilized friction angle of the natural soil, a 3D slope stability analysis was performed using the slope geometry shown in Fig. 12, and a cohesion of zero for the natural soil. Shear resistance along the vertical sides

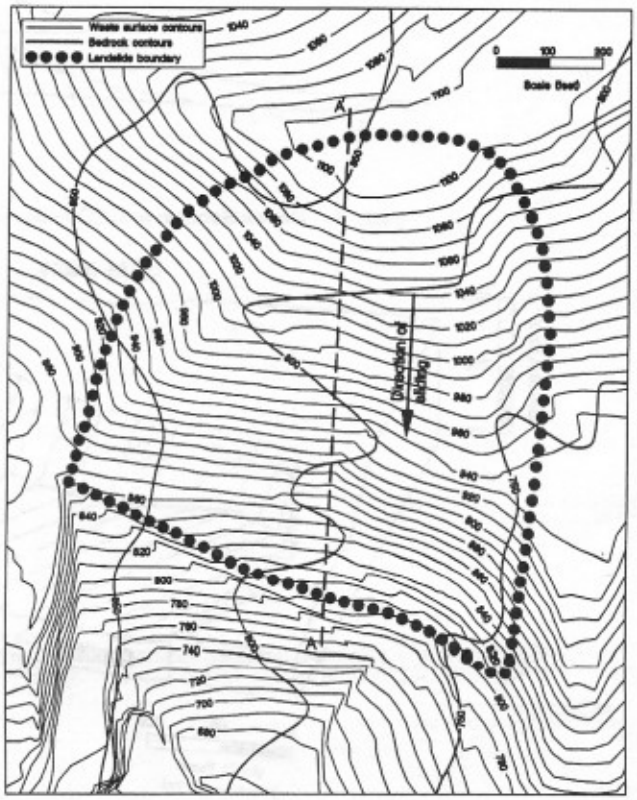

FIG. 10. Plan View of Cincinnati Landfill Failure

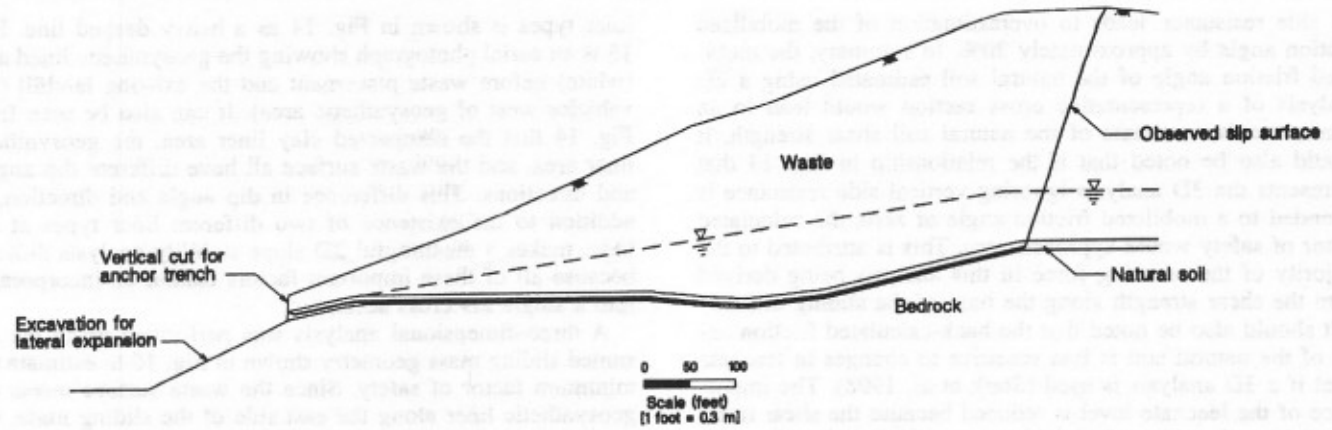

FIG. 11. Cross Section and 2D Failure Surface of Cincinnati Landfill Failure (Section A-A')

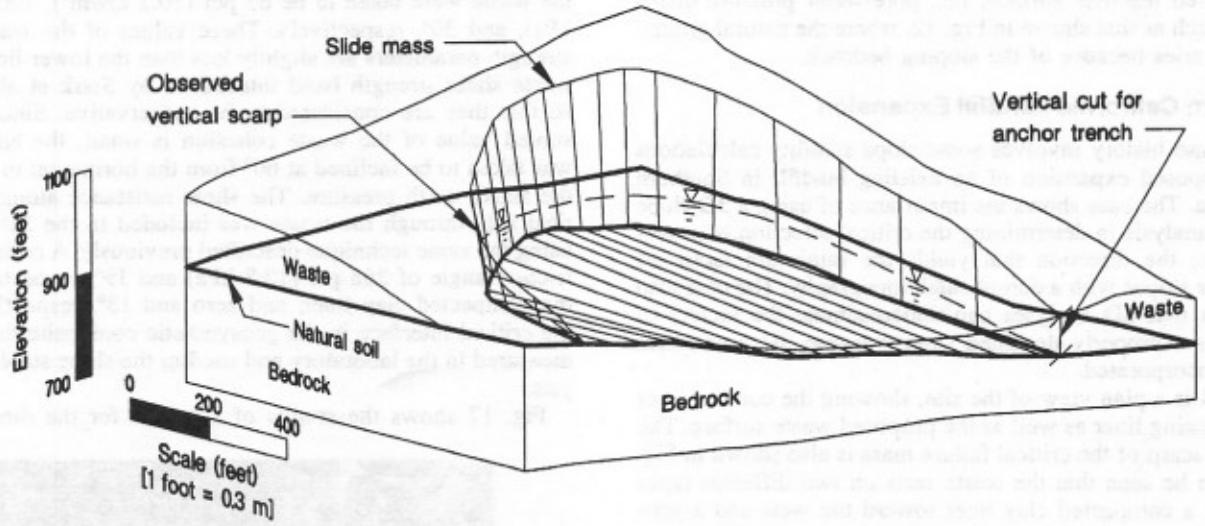

FIG. 12. 3D View of Slide Mass for Cincinnati Landfill Failure

was considered using the same technique described before. The cohesion for the imaginary layer was calculated as follows:

$$c_i' = c' + k_0 \sigma_v' \tan \phi' \tag{3}$$

where c' and ϕ' = cohesion and friction angle of the solid waste; σ_v' = average vertical effective stress over the depth of the sliding mass side; and k_0 = coefficient of earth pressure at rest for the solid waste ($k_0 = 1 - \sin \phi'$).

Because of the large difference between the shear strength of the waste and the natural soil, analyses of representative 2D cross sections showed that underestimation of the factor of safety due to using Janbu's simplified method exceeds overestimation of the factor of safety caused by ignoring the nonlinearity of the natural soil failure envelope by approximately 7%. Consequently, this percentage is used to increase the calculated 3D factors of safety using Janbu's simplified method and linear failure envelopes. The results of the 3D analysis are shown in Fig. 13. It can be seen that if the side resistance is considered, the back-calculated or mobilized friction angle of the natural soil is approximately 10°. This value is in agreement with the drained residual friction angle of representative samples tested using the procedure described by Stark and Eid (1993). The tested specimen has a liquid limit, plastic limit, and clay-size fraction of 69, 28, and 55%, respectively. A drained residual shear strength condition was probably mobilized for the natural soil in this case for a number of reasons, including the strain incompatibility between the waste and natural soil (Stark et al. 1998).

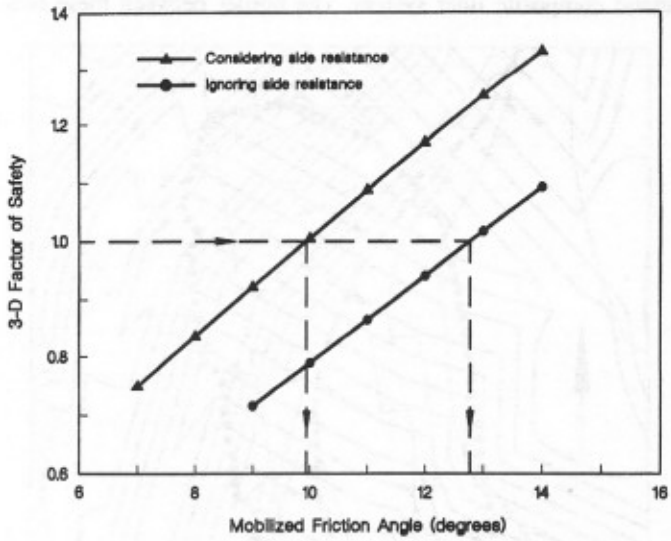

FIG. 13. Mobilized Friction Angle and Associated 3D Factors of Safety for Cincinnati Landfill Failure

Fig. 13 also presents the 3D factors of safety and the associated back-calculated friction angles of the natural soil if the side resistance is not considered, i.e., similar to the 2D condition. This analysis is not a true 2D analysis because the entire slide mass is considered instead of a single cross section. As a result, this analysis provides a factor of safety that is in between a 3D and 2D analysis. It can be seen that ignoring

the side resistance leads to overestimation of the mobilized friction angle by approximately 30%. In summary, the mobilized friction angle of the natural soil estimated using a 2D analysis of a representative cross section would lead to an unconservative estimate of the natural soil shear strength. It should also be noted that if the relationship in Fig. 13 that represents the 3D analysis ignoring vertical side resistance is extended to a mobilized friction angle of zero, the calculated factor of safety would approach zero. This is attributed to the majority of the resisting force in this analysis being derived from the shear strength along the base of the sliding mass.

It should also be noted that the back-calculated friction angle of the natural soil is less sensitive to changes in leachate level if a 3D analysis is used (Stark et al. 1998). The importance of the leachate level is reduced because the shear resistance along the sides of the slide mass is included in the analysis. In addition, a 3D analysis is able to accommodate a complicated leachate surface, i.e., pore-water pressure distribution, such as that shown in Fig. 12, where the natural ground surface varies because of the sloping bedrock.

Southern California Landfill Expansion

This case history involves some slope stability calculations for a proposed expansion of an existing landfill in Southern California. The case shows the importance of using a 3D slope stability analysis in determining the critical direction of movement, i.e., the direction that yields the minimum factor of safety, for slopes with a complicated topography. The case also illustrates that 2D analyses can underestimate the factors of safety for a properly designed slope because 3D kinematics are not incorporated.

Fig. 14 is a plan view of the site, showing the contour lines of the existing liner as well as the proposed waste surface. The potential scarp of the critical failure mass is also shown in Fig. 14. It can be seen that the waste rests on two different types of liners; a compacted clay liner toward the west and a geosynthetic composite liner system toward the east. New regulations require the expansion area to be lined with a geosynthetic composite liner system. The border between these two liner types is shown in Fig. 14 as a heavy dashed line. Fig. 15 is an aerial photograph showing the geosynthetic lined area (white) before waste placement and the existing landfill (see vehicles west of geosynthetic area). It can also be seen from Fig. 14 that the compacted clay liner area, the geosynthetic liner area, and the waste surface all have different dip angles and directions. This difference in dip angle and direction, in addition to the existence of two different liner types at the base, makes a meaningful 2D slope stability analysis difficult because all of these important factors cannot be incorporated into a single 2D cross section.

A three-dimensional analysis was performed using the assumed sliding mass geometry shown in Fig. 16 to estimate the minimum factor of safety. Since the waste surface meets the geosynthetic liner along the east side of the sliding mass, the west side provides the largest contribution to the sliding resistance. The moist unit weight, cohesion, and friction angle of the waste were taken to be 65 pcf (10.2 kN/m^3), 100 psf (4.8 kPa), and 30°, respectively. These values of the waste shear strength parameters are slightly less than the lower limit of the waste shear strength band introduced by Stark et al. (1998), so that they are considered to be conservative. Since the assumed value of the waste cohesion is small, the back scarp was taken to be inclined at 60° from the horizontal to simulate the active earth pressure. The shear resistance along the vertical side through the waste was included in the 3D analysis using the same technique described previously. A cohesion and friction angle of 268 psf (12.8 kPa) and 19°, respectively, for the compacted clay liner, and zero and 13°, respectively, for the critical interface in the geosynthetic composite liner, were measured in the laboratory and used in the slope stability analysis.

Fig. 17 shows the results of a search for the direction of

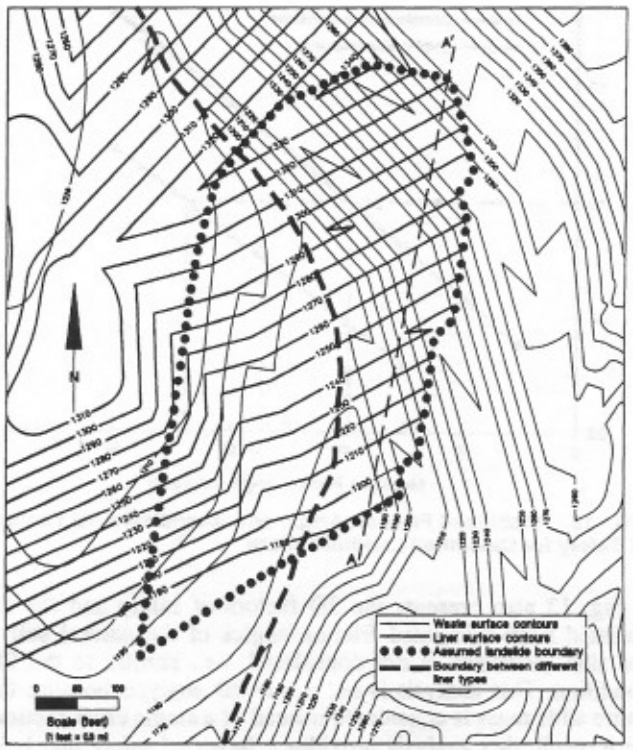

FIG. 14. Plan View for California Landfill Expansion

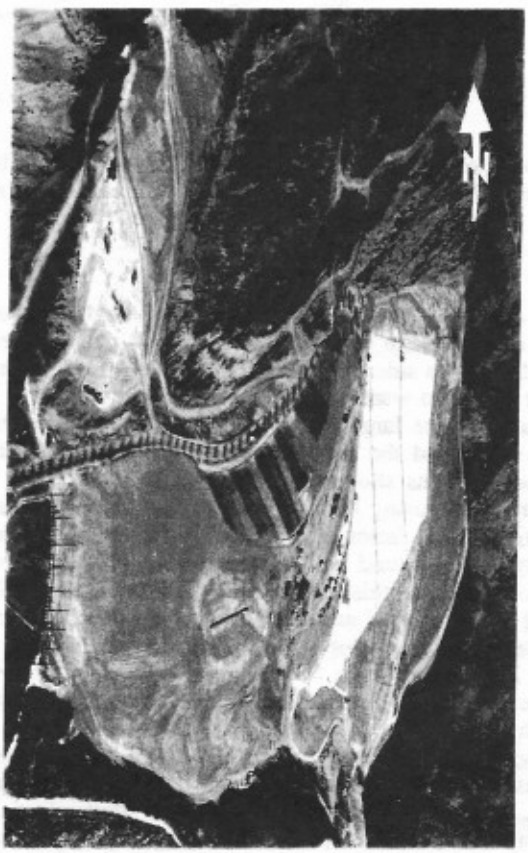

FIG. 15. Aerial View of California Landfill Expansion with Geosynthetic Lined Area Shown in White and Existing Landfill Directly West; Note Vehicles on Existing Landfill (Photo Courtesy of Damon Brown, EBA Wastechnologies, Inc.)

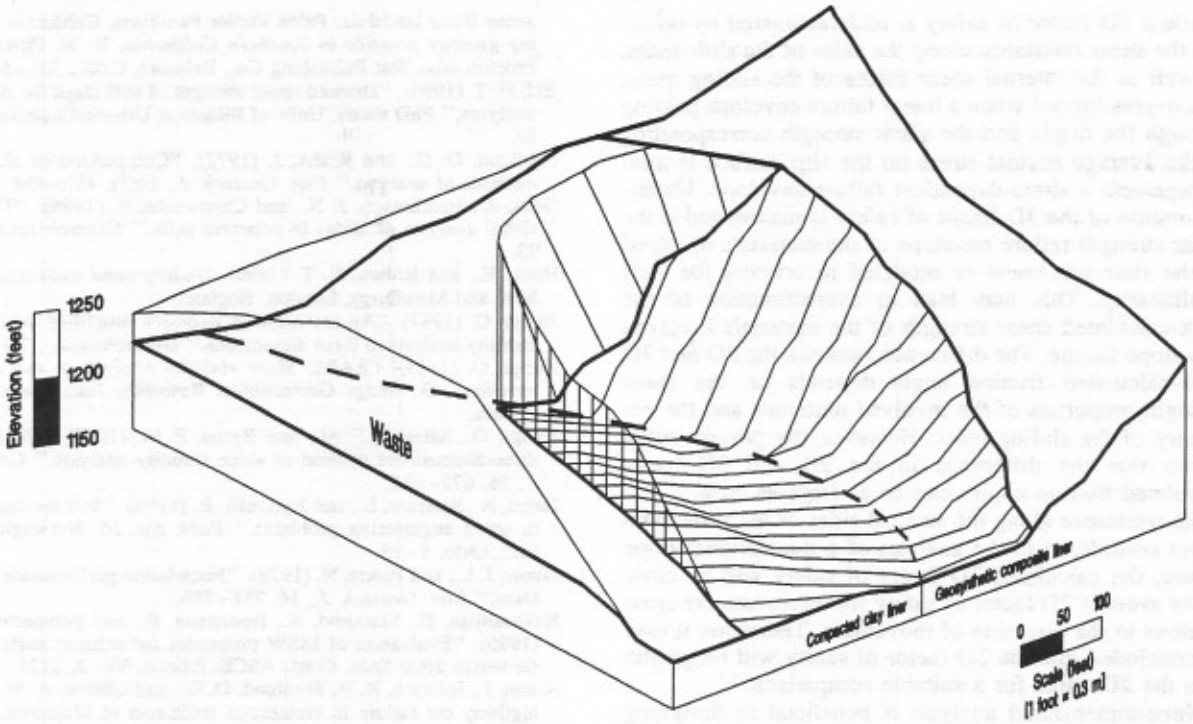

FIG. 16. 3D View of Assumed Sliding Mass for California Landfill

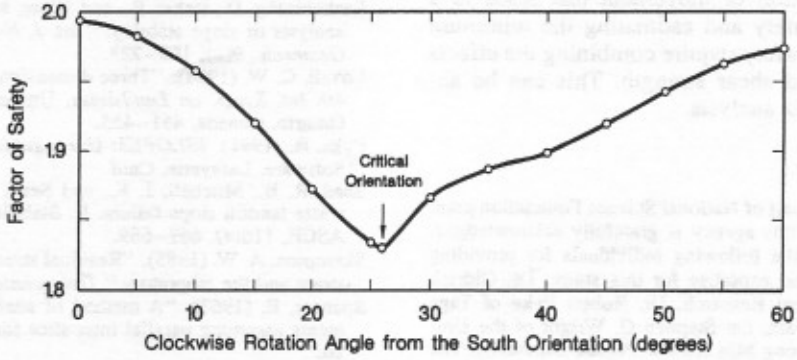

FIG. 17. Search for Critical Sliding Direction

sliding that yields the minimum 3D factor of safety. It can be seen that a minimum factor of safety of 1.83 occurs at a direction of 26° clockwise from the south direction. This direction probably reflects a weighted average between the different base dip angles and directions with their associated areas and shear strengths, and the potential failure surface. A 2D slope stability analysis cannot consider the combined effect of these factors. As a result, a 3D analysis can be used to analyze the stability of slopes with complicated topography, variable basal shear strengths, and site conditions similar to those in this case.

Smaller sliding masses were also considered during the analysis of this landfill expansion. An example of these masses is one that is in between cross section A-A′ and the eastern limit of waste in Fig. 14. This slide mass was thought to be critical because of the lack of sliding resistance along the eastern side and the resulting 2D factor of safety of 0.97 for cross section A-A′. However, a 3D analysis for sliding in the direction of cross section A-A′ yielded a factor of safety of 1.65 for this slide mass. The high 3D factor of safety was attributed to including the shear resistance along a vertical surface through the waste at the west side of the potential slide mass. This also emphasizes the importance of considering the 3D behavior in slope stability analyses involving materials that exhibit a large difference in shear strength.

CONCLUSIONS

The following conclusions are based on two- and three-dimensional slope stability analyses of field case histories and a representative slope model:

1. Sides of sliding masses in translational failures are usually vertical, which leads to a minimum amount of shear resistance being mobilized along these sides. Even with the minimum amount of side resistance being mobilized, slopes failing in a translational mode exhibit the most pronounced difference between 2D and 3D factors of safety because of the large difference between the mobilized shear strength along the back scarp and sides of the slide mass and that along the base.
2. Commercially available 3D slope stability software has inherent limitations that affect the calculated factor of safety for a translational failure mode. These limitations include ignoring the shear resistance along the vertical sides of the sliding mass, modeling a nonlinear failure envelope with a linear failure envelope, and using a 3D slope stability method that ignores some of the internal shear forces. A technique is presented to overcome some of these limitations and provide a better estimate of the 3D factor of safety.

3. While a 3D factor of safety is underestimated by ignoring the shear resistance along the sides of the slide mass, as well as the internal shear forces of the sliding mass, it is overestimated when a linear failure envelope passing through the origin and the shear strength corresponding to the average normal stress on the slip surface is used to represent a stress-dependent failure envelope. Underestimation of the 3D factor of safety is maximized if the shear strength failure envelope of the materials involved in the slide are linear or modeled to account for their nonlinearity. This may lead to overestimation of the back-calculated shear strength of the materials involved in a slope failure. The difference between the 2D and 3D back-calculated friction angle depends on the shear strength properties of the involved materials and the geometry of the sliding mass. However, the present study shows that the difference in the 2D and 3D back-calculated friction angles can be as large as 30%.
4. If the resistance along the vertical sides of the slide mass is not considered in the analysis of a translational slope failure, the calculated 3D factor of safety will be close to the average 2D factor of safety for representative cross sections in the direction of movement. Therefore, it may be concluded that the 3D factor of safety will be greater than the 2D value for a suitable comparison.
5. A three-dimensional analysis is beneficial in designing slopes with a complicated topography, shear strength, and/or pore-water pressure condition. For these cases, determining the direction of movement that leads to a minimum factor of safety and estimating the minimum value of the factor of safety require combining the effects of slope geometry and shear strength. This can be accomplished using a 3D analysis.

ACKNOWLEDGMENTS

This study was performed as part of National Science Foundation grant BCS-93-00043. The support of this agency is gratefully acknowledged. The writers also acknowledge the following individuals for providing their slope stability software and expertise for this study: Dr. Oldrich Hungr of O. Hungr Geotechnical Research, Dr. Robert Pyke of Taga Engineering Systems and Software, Dr. Stephen G. Wright of the University of Texas at Austin, and Jong Min Kim of Purdue University. The review comments provided by Dr. Dov Leshchinsky of the University of Delaware are also appreciated. Damon Brown and Steve Huvane of EBA Wastechnologies, Santa Rosa, California, provided the information and photograph for the landfill expansion case history.

APPENDIX. REFERENCES

Baligh, M. M., and Azzouz, A. S. (1975). "End effects of stability of cohesive slopes." *J. Geotech. Engrg. Div.*, ASCE, 101(11), 1105–1117.

Beene, R. R. W. (1967). "Waco Dam slide." *J. Soil Mech. and Found. Div.*, ASCE, 93(4), 35–44.

Bishop, A. W. (1955). "The use of the slip circle in the stability analysis of slopes." *Geotechnique*, 5(1), 7–17.

Byrne, R. J., Kendall, J., and Brown, S. (1992). "Cause and mechanism of failure, Kettleman Hills Landfill B-19, Unit IA." *Proc., Stability and Perf. of Slopes and Embankments-II*, ASCE, Reston, Va., 2, 1188–1215.

Cavounidis, S. (1987). "On the ratio of factors of safety in slope stability analysis." *Geotechnique*, 37(2), 207–210.

Chen, R. H. (1981). "Three-dimensional slope stability analysis." *Rep. JHRP-81-17*, Purdue Univ., West Lafayette, Ind.

Chen, R. H., and Chameau, J.-L. (1983). "Three-dimensional limit equilibrium analysis of slopes." *Geotechnique*, 32(1), 31–40.

Ching, R., and Fredlund, D. G. (1984). "Quantitative comparison of limit equilibrium methods of slices." *Proc., 4th Int. Symp. on Landslides*, University of Toronto Press, Toronto, Ontario, Canada, 373–379.

Duncan, J. M. (1992). "State-of-the-art: Static stability and deformation analysis." *Proc., Stability and Perf. of Slopes and Embankments-II*, ASCE, Reston, Va. 1, 222–266.

Ehlig, P. L. (1992). "Evolution, mechanics and mitigation of the Portuguese Bend landslide, Palos Verdes Peninsula, California." *Engineering geology practice in Southern California*, B. W. Pipkin and R. J. Proctor, eds., Star Publishing Co., Belmont, Calif., 531–553.

Eid, H. T. (1996). "Drained-shear strength of stiff clays for slope stability analyses," PhD thesis, Univ. of Illinois at Urbana-Champaign, Urbana, Ill.

Fredlund, D. G., and Krahn, J. (1977). "Comparison of slope stability methods of analysis." *Can. Geotech. J.*, 14(3), 429–439.

Gens, A., Hutchinson, J. N., and Cavounidis, S. (1988). "Three-dimensional analysis of slides in cohesive soils." *Geotechnique*, 38(1), 1–23.

Hoek, E., and Brown, E. T. (1980). *Underground excavations.* Inst. of Min. and Metallurgy, London, England.

Hungr, O. (1987). "An extension of Bishop's simplified method of slope stability analysis to three dimensions." *Geotechnique*, 37(1), 113–117.

Hungr, O. (1988). *CLARA: Slope stability analysis in two or three dimensions.* O. Hungr Geotechnical Research, Inc., Vancouver, B.C., Canada.

Hungr, O., Salgado, F. M., and Byrne, P. M. (1989). "Evaluation of a three-dimensional method of slope stability analysis." *Can. Geotech. J.*, 26, 679–686.

Janbu, N., Bjerrum, L., and Kjaernsli, B. (1956). "Soil mechanics applied to some engineering problems." *Publ. No. 16*, Norwegian Geotech. Inst., Oslo, 5–26.

Jasper, J. L., and Peters, N. (1979). "Foundation performance of Gardiner Dam." *Can. Geotech. J.*, 16, 758–788.

Kavazanjian, E., Matasovi, N., Bonaparte, R., and Schmertmann, G. R. (1995). "Evaluation of MSW properties for seismic analysis." *Proc., Geoenvir. 2000 Spec. Conf.*, ASCE, Reston, Va., 2, 1126–1141.

Krahn, J., Johnson, R. F., Fredlund, D. G., and Clifton, A. W. (1979). "A highway cut failure in cretaceous sediments at Maymont, Saskatchewan." *Can. Geotech. J.*, 16, 703–715.

Leshchinsky, D., and Baker, R. (1986). "Three-dimensional slope stability: End effects." *Soils and Found.*, 26(4), 98–110.

Leshchinsky, D., Baker, R., and Silver, M. L. (1985). "Three dimensional analysis of slope stability." *Int. J. Numer. and Analytical Methods in Geomech.*, 9(2), 199–223.

Lovell, C. W. (1984). "Three dimensional analysis of landslides." *Proc., 4th Int. Symp. on Landslides*, University of Toronto Press, Toronto, Ontario, Canada, 451–455.

Pyke, R. (1991). *TSLOPE3: Users guide.* Taga Engineering Systems and Software, Lafeyette, Calif.

Seed, R. B., Mitchell, J. K., and Seed, H. B. (1990). "Kettleman Hills waste landfill slope failure. II: Stability analysis." *J. Geotech. Engrg.*, ASCE, 116(4), 669–689.

Skempton, A. W. (1985). "Residual strength of clays in landslides, folded strata and the laboratory." *Geotechnique*, 35(1), 3–18.

Spencer, E. (1967). "A method of analysis of the stability of embankments assuming parallel inter-slice forces." *Geotechnique*, 17(1), 11–26.

Stark, T. D., and Eid, H. T. (1992). "Comparison of field and laboratory residual shear strengths." *Proc., Stability and Perf. of Slopes and Embankments-II*, ASCE, Reston, Va., 876–889.

Stark, T. D., and Eid, H. T. (1993). "Modified Bromhead ring shear apparatus." *ASTM Geotech. J.*, 16(1), 100–107.

Stark, T. D., and Eid, H. T. (1994). "Drained residual strength of cohesive soils." *J. Geotech. Engrg.*, ASCE, 120(5), 856–871.

Stark, T. D., and Eid, H. T. (1997). "Slope stability analyses in stiff fissured clays." *J. Geotech. and Geoenvir. Engrg.*, ASCE, 123(4), 335–343.

Stark, T. D., Eid, H. T., Evans, W. D., and Sherry, P. E. (1998). "Solid waste slope failure." *J. Geotech. and Geoenvir. Engrg.*, ASCE, in press.

Stark, T. D., and Poeppel, A. R. (1994). "Landfill liner interface strengths from torsional ring shear tests." *J. Geotech. Engrg.*, ASCE, 120(3), 597–615.

Stark, T. D., Williamson, T. A., and Eid, H. T. (1996). "HDPE geomembrane/geotextile interface shear strength." *J. Geotech. Engrg.*, ASCE, 122(3), 197–203.

Thomaz, J. E. (1986). "A general method for three dimensional slope stability analysis." *Information Rep. JHRP-86-4*, Purdue Univ., West Lafayette, Ind.

Thomaz, J. E., and Lovell, C. W. (1988). "Three dimensional slope stability analysis with random generation of surfaces." *Proc., 5th Int. Symp. on Landslides*, 1, 777–781.

Ugai, K. (1988). "Three-dimensional slope stability analysis by slice methods." *Proc., 6th Int. Conf. on Numer. Methods in Geomech.*, A. A. Balkema, Rotterdam, The Netherlands, 1369–1374.

Wright, S. G. (1992). *UTEXAS3: A computer program for slope stability calculations.* Geotech. Engrg. Software GS86-1, Dept. of Civ. Engrg., Univ. of Texas, Austin.

Wright, S. G., and Duncan, J. M. (1972). "Analyses of Waco Dam slide." *J. Soil Mech. and Found. Div.*, ASCE, 98(9), 869–877.